Numerical study of electromagnetic waves interacting with negative index materials

Pavel Kolinko and David R. Smith

Department of Physics, University of California, San Diego, CA 92037-0319 USA
drs@sdss.ucsd.edu

http://physics.ucsd.edu/~drs

Abstract: We study numerically the electromagnetic scattering properties of structures with negative indices of refraction. To perform this analysis, we utilize a commercial finite-element based electromagnetic solver (HFSS, Ansoft), in which a negative index material can be formed from mesh elements whose permittivity and permeability are both negative. In particular, we investigate the expected transmission characteristics of a finite beam incident on negative index prisms and lenses. We also confirm numerically the predicted superlens effect of an image formed by a planar slab with index n=-1, using two subwavelength ($\lambda/20$) slits as objects.

OCIS codes: (260.0260) Physical optics; (080.0080) Geometrical optics

References and links

1. V. G. Veselago "The electrodynamics of substances with simultaneously negative values of ε and μ," Soviet Physics USPEKI **10**, 509 (1968).
2. J. B. Pendry, "Electromagnetic materials enter the negative age," Physics World **14**, 47 (2001).
3. D. R. Smith, N. Kroll, "Negative refractive index in left-handed materials," Phys. Rev. Lett. **85**, 2933 (2000).
4. D. R. Smith, Willie J. Padilla, D. C. Vier, S. C. Nemat-Nasser, S. Schultz, "A composite medium with simultaneously negative permeability and permittivity," Phys. Rev. Lett. **84,** 4184 (2000).
5. R. Shelby, D. R. Smith, S. Schultz, "Experimental verification of a negative index of refraction," Science **292**, 77 (2001).
6. J. B. Pendry, "Negative refraction makes a perfect lens," Phys. Rev. Lett. **85**, 3966 (2000).
7. C. Caloz, C.-C. Chang, T. Itoh, "Full-wave verification of the fundamental properties of left-handed materials in waveguide configurations," J. App. Phys. **90**, 5483 (2001).
8. C. Parazzoli, R. B. Greegor, K. Li, B. E. C. Kotenbah and M. Tanelian, "Experimental verification and simulation of negative index of refraction using Snell's law," Phys. Rev. Lett. submitted (2002).
9. A. Yariv, *Optical electronics in modern communications, fifth Ed.* (Oxford Press, 2000), Chap. 2.
10. N. Garcia and M. Nieto-Vesperinas, "Left-handed materials do not make a perfect lens," Appl. Phys. Lett. **88**, 207403 (2002).
11. R. W. Ziolkowski, E. Heyman, "Wave propagation in media having negative permittivity and permeability," Phys. Rev. E **64**, 056625 (2001).
12. J. T. Shen, P. M. Platzman, "Near field imaging with negative dielectric constant lenses," Appl. Phys. Lett. **80**, 3286 (2002).
13. D. R. Smith *et al.,* "Limitations on sub-diffraction imaging with a negative index slab," Appl. Phys. Lett. in press (2003).
14. R. Ruppin, "Surface polaritons of a left-handed materials slab," J. Phys.: Condens. Matter **13**, 1811 (2001).

#1998 - $15.00 US
Received January 17, 2003; Revised March 09, 2003

1. Introduction

The index-of-refraction is a simple and commonly used means of characterizing the optical properties of a material. Knowledge of the indices-of-refraction of two continuous and isotropic materials, for example, is sufficient to predict the refraction angle of a beam incident at the interface between the two materials.

In all known naturally occurring materials, the real part of the index-of-refraction is positive. However, this is not a fundamental restriction, as was pointed out in an early paper by V. G. Veselago [1], who suggested that a material could exist that would exhibit an index-of-refraction whose real part was negative. Were a beam to undergo refraction at the interface between two materials, one of which possessed a negative index and the other positive, the transmitted wave would be refracted to the *same* side of the surface normal as the incident wave, rather than the *opposite* side.

Veselago discovered the possibility of negative refraction via a theoretical exploration of "left-handed" materials—materials whose electrical permittivity (ε) and magnetic permeability (μ) are simultaneously negative. In analyzing plane waves propagating in left-handed materials, Veselago noted that the phase and group velocities were reversed, giving rise to a significant modification of numerous electromagnetic properties, including the change in sign of the refractive index. The prospect of a negative refractive index might at first be considered surprising, since the form of the refractive index, given by $n = \sqrt{\varepsilon\mu}$, would appear to be unchanged whether ε and μ are both positive or both negative. However, analytical arguments based on causality show that, in fact, the negative square root of the index must be taken for a left-handed material [2, 3].

Since left-handed materials or compounds do not exist in nature, the discussion of left-handed materials was not particularly relevant; in fact, the topic was not further pursued until recently, when it was demonstrated that artificially structured left-handed metamaterials could be constructed [4]. Such materials have been used to demonstrate negative refraction experimentally at microwave frequencies [5], thus motivating further research into the possibilities that negative index materials might provide. Even the simplest configurations of negative index materials, which can be analyzed by analytical methods, have yielded surprising results [1, 6], indicating there is much to discover in this new field.

Here we investigate numerically the scattering of electromagnetic waves from negative index materials using commercial simulation software (HFSS, Ansoft Corporation, Pittsburgh, PA, USA). While negative refraction has been observed only in artificial structures composed of macroscopic scattering elements that are nevertheless small compared to the wavelength of the radiation of interest, it is a useful first step to study *continuous* negative index materials, which are amenable to numerical simulation. Since negative index materials require both negative ε and μ, implying frequency dispersion, a time-domain simulation would require specification of the frequency dependence of the material parameters. An alternate approach is to utilize the driven solution in HFSS, in which a steady-state scattering calculation including negative index regions can be performed at a single frequency without the specification of the frequency dependence of ε and μ.

HFSS solves Maxwell's equations using a finite element method, in which the solution domain is divided into tetrahedral elements, termed a "mesh." The characteristics of the generated mesh are crucial to obtaining a reliable, well-converged solution. In the calculations performed in this paper, we have utilized a combination of manual seeding to generate the initial mesh, followed by successive iterations where the mesh density is increased adaptively. The initial mesh usually contained 5,000-10,000 tetrahedra. After twenty-five or so iterations, the final mesh typically contained ~100,000 tetrahedra. Convergence was assessed by monitoring the convergence of the S-parameters (*i.e.*, transmission and reflection) from iteration to iteration. This determination of convergence is global, so that local errors can still be present in the computed fields; however, unphysical

#1998 - $15.00 US Received January 17, 2003; Revised March 09, 2003

anomalies are usually distinguishable by inspection of the field plots, and changes in meshing or number of tetrahedral can be made to improve convergence.

HFSS simulations have been previously performed to investigate the behavior of guided electromagnetic waves with negative index materials [7]. In contrast, we present here simulations in which the electromagnetic waves, unrestricted in two dimensions, undergo scattering from negative index structures. For specific examples, we study refraction from a negative index wedge (Section 2), a focusing slab (Section 3), and a negative index focusing lens (Section 4).

2. Refraction from a wedge

The index of refraction of a material can be experimentally determined by observing the angle of deflection of a beam through a prism composed of the material. This approach has been taken in recent experimental demonstrations in both a two-dimensional scattering chamber [4], as well as in free space [8]. The two-dimensional geometry is particularly useful for proof-of-principle demonstrations, as the fabrication, computational and experimental burdens are significantly reduced. The calculations we present in this paper are all based on the two-dimensional geometry with the electric field polarized orthogonal to the plane of incidence (i.e., s-polarization).

In the published experiment on a two-dimensional wedge sample, two circular, conducting plates spaced 1 cm apart were used to form a two-dimensional waveguide structure. An incident beam was formed by guiding waves between two walls of microwave absorber which gradually tapered to form an aperture of 10 cm. A wedge sample was placed across this aperture, such that the incident beam entered the medium at normal incidence, undergoing refraction at the second interface. The refraction angle at the second surface was 18.43°. The refracted power as a function of angle was then measured, with the index being determined from a straight-forward application of Snell's law.

Figure 1 shows the computed field intensity for an incident beam refracting from a wedge sample with similar parameters as the experimental sample. The field intensity distribution is shown at the midplane between two electric boundary conditions spaced 1 cm apart. Superimposed lines provide an indication of the absorber and sample locations. Figure 1(a) shows the refraction from a sample with ε=2.2, corresponding roughly to the Teflon sample used as a control in the experiments. The surface normal is shown by the black line in the figure. The peak of the refracted beam occurs at an angle of 25.6° from the incident beam direction, indicating a refractive index of n=1.414, consistent with the dielectric constant used. Figure 1(b) shows the refraction from a sample with ε=-1 and μ=-1. We see that the angle of the peak refracted power is clearly in the "negative" direction with respect to the surface normal, corresponding to the expected refractive index of n=-1. Note also that the case of $\varepsilon=\mu=-1$ represents a perfect impedance match (z=+1) to free space, for all angles of incidence; thus, the field pattern in the case of the left-handed material exhibits minimal reflection at the wedge interfaces as compared with Fig. 1(a).

A plot the field intensity as a function of angle at a radius of 14.9 cm away from the center point of the wedge, indicated with a black dot on Fig. 1(a), is shown in Fig. 2. The width of the beam is set by the aperture dimension (6 cm) and diffraction. As the beam emerges from the aperture, the angular field pattern of the intensity initial evolves as a function of propagation distance until a final asymptotic distribution is reached. The characteristic distance over which the behavior transitions to the asymptotic limit is given by a constant multiplied by d^2/λ (for a three-dimensional beam) [9]. The angular profile of the field intensity was thus mapped at a radius somewhat within the non-asymptotic region, similar to where energy was detected in the experimental apparatus [4]. The computational requirements to perform the calculation further away from the aperture increase considerably as the radius is increased, making it impractical to achieve results beyond what we have shown in Fig. 2. However, given the complete field specification along a plane just after the wedge, it is possible to compute the expected far-field pattern. In similar calculations, it has

#1998 - $15.00 US Received January 17, 2003; Revised March 09, 2003

been shown that the difference between the detected intensity in this region versus that in the far-zone is minor, and does not change conclusions as to the refraction angle [8].

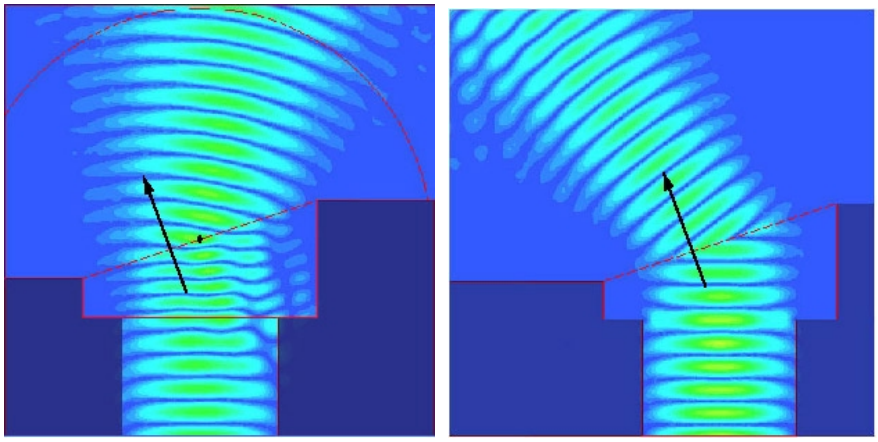

Fig. 1. (a) (740K) Movie of an incident beam (from below) positively refracted by a wedge sample with ε=2.2 and μ=+1. The darkened regions indicate absorber, in analogy with the experiments. The circle indicates the path along which the field plots in Fig. 2 were taken. (b) (682K) Movie showing negative refraction from a wedge with ε=-1 and μ=-1.

The unit cell in the experimental samples used to date has been roughly a factor of six smaller than the wavelength. With so large an inherent discretization, the refraction interface of the wedge rather than being smooth actually has a staircase pattern, as indicated in Fig. 3. The nonuniform refraction interface leads to some minor distortion of the field within the wedge, as well as introducing a secondary beam. While the effects somewhat more significant in the case of the negative index material, the main refracted beam still lies in the expected direction.

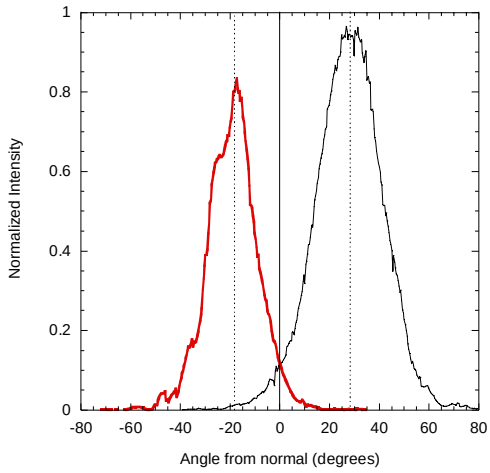

Fig. 2. Angular plots of the field intensity of the refracted wave at a constant radius away from a positive index wedge with ε=2.2 and μ=+1 (black curve), and a negative index wedge with ε=-1 and μ=-1 (red cruve). The dashed lines indicate the expected refraction angles as predicted by Snell's law based on the refractive index of the materials.

#1998 - $15.00 US
Received January 17, 2003; Revised March 09, 2003

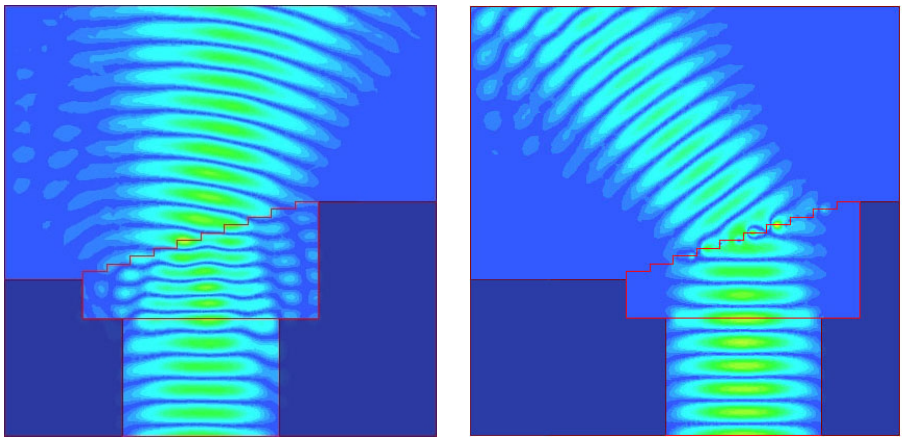

Fig. 3. (a) (779 KB) Movie of an incident beam (from below) positively refracted by a wedge sample with ε=2.2 and μ=+1. (b) (662 KB) Movie showing negative refraction from a wedge with ε=-1 and μ=-1. In both cases, a stepped pattern was introduced along the refracting interface to simulate more closely the samples used in the experimental work.

3. Sub-diffraction limited focusing

One of the most stimulating developments of negative index media has been the prospect of near-field focusing, as suggested by Pendry [5]. Veselago initially showed that a localized electromagnetic source distribution incident on a finite-thickness slab of material with ε=-1 and μ=-1 would be refocused at a plane on the other side of the slab. However, Pendry noted that not only would the propagating components be recovered in the image, the non-propagating evanescently decaying components could also be recovered as well. These evanescent components—always lost in conventional optics—are responsible for the resolution beyond the diffraction limit. Using a negative index material as a lens can reconstitute the evanescent fields, and so provide "perfect" imaging of features much smaller than the wavelength of illumination.

The suggestion of superfocusing has proven controversial [10], and initial attempts to observe the effect via numerical simulations did not produce definitive results [11]. By carefully analyzing the dependence of the superresolution as a function of deviation of the material parameters from the ideal condition, other authors have shown that the superfocusing effect should indeed be realizable, but only over a particularly restrictive range of slab parameters [12, 13].

To demonstrate the superfocusing effect here, we have used a slab one-tenth of a wavelength in thickness, with a double slit acting as the object. These dimensions were chosen to be consistent with the parameter range for which significant subwavelength focusing should be possible [13]. The double slit is used here to differentiate the resolution from other effects in the image plane that may result when a subwavelength apertured source excites surface modes on a planar slab. The field patterns associated with the double-slit source without and with a positive index (ε=2.2) slab are shown in Figs. 4(a) and 4(b), respectively. The source consists of an absorbing material (ε=μ=1, ε"=0.1) with two subwavelength slits, λ/20 in size, spaced a distance of λ/10 apart (center-to-center). Either with or without the positive index slab, the diffraction patterns from the two slits merge so that the sub-wavelength information is lost rapidly with distance from the object plane. When a negative index slab with ε=μ=-1 is inserted, however, two "hot spots" appear on the far surface of the slab, as shown in Fig 4(c). In agreement with the predictions of Pendry [4], the increased field intensity is due to the decay of the near-fields being reversed; a distance of λ/10 beyond the far surface of the slab, the field distribution approximates the object field distribution.

#1998 - $15.00 US Received January 17, 2003; Revised March 09, 2003

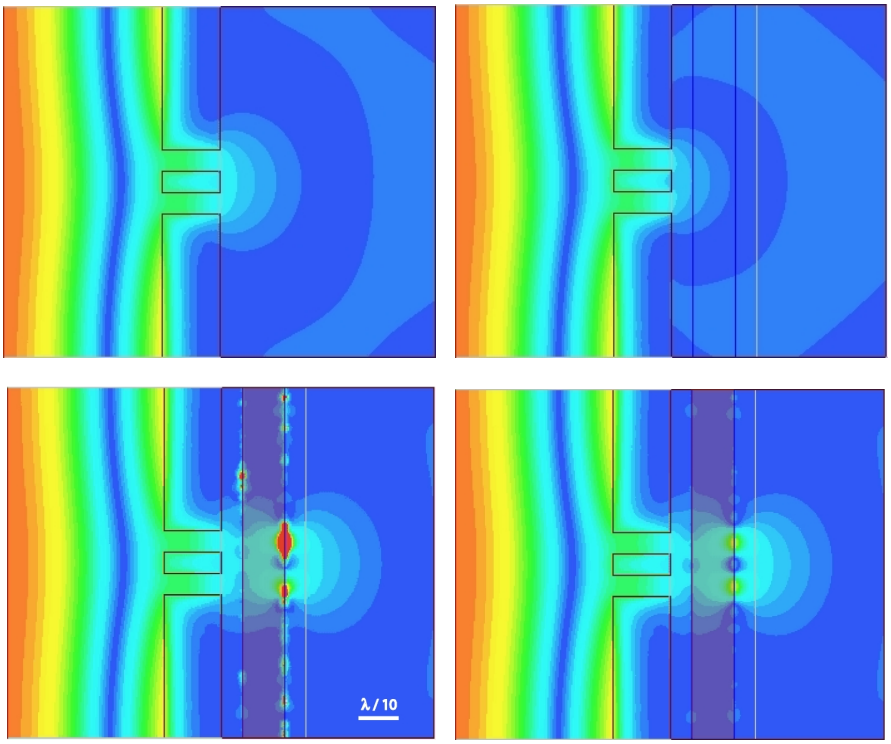

Fig. 4. (595 KB) Movie of a plane wave (incident from the left) mostly reflected from an absorbing plane. Two slits separated by a distance of λ/10, and of width λ/20, admit a small portion of the radiation, forming a subwavelength source field distribution. (a) With no slab present, all subwavelength information is lost a short distance away from the slits. (b) With a positive index slab (ε=2.2), indicated by the continuous black lines, no subwavelength information is transmitted at the image plane (continuous white line). (c) A slab with ε=-1 and μ=-1 refocuses the field distribution from the object plane, including subwavelength information; however, unwanted surface modes appear on the slab surfaces. (d) (657 KB) Movie showing that the introduction of losses (ε"=μ"=0.001) damps the surface modes while retaining most of the resolution.

Note that the perfect lens configuration gives rise to extra (and uneven) surface mode excitations that run along the length of both sides of the slab. These extra excitations are not present in the perfect lens theory, but reflect the inherent inaccuracy of the finite element program to simulate a continuous material. As has been shown by several authors, any deviation from the ideal conditions, in either material parameters or "graininess" of the material caused by meshing, for example, will lead to the excitation of unwanted surface modes [13], whose properties have been investigated in detail for the slab geometry [14]. The introduction of a small amount of loss (ε" and μ") limits the resolution of the image, but also damps the unwanted surface modes, as shown in Fig. 4(d).

A plot of the field intensity across the image plane is shown in Fig. 5 for four different cases. For comparison, the object field distribution is shown as the black dashed line, taken along the plane just at the exit of the slits. With either free space (not shown) or a positive index slab (ε=2.2, gray curve) the near fields decay rapidly, leaving a diffraction-limited field distribution at the position of the image plane. When a negative index slab (ε=μ=-1+0.001i) is inserted, however, the object field distribution is reproduced at the image plane on the far side of the slab (solid black curve).

#1998 - $15.00 US
Received January 17, 2003; Revised March 09, 2003

Deviations from the near-ideal condition degrade the performance of the lens. The introduction of increased material losses (ε=μ=-1+0.1i), for example, results in a loss of the subwavelength information, as indicated by the green curve in Fig. 5. As has been previously noted [6], not all deviations from the ideal case degrade the image as severely; for the s-polarization we analyze here, the image is not seriously reduced even for the value of ε=1, as shown by the red curve in Fig. 5. This insensitivity to such a significant perturbation in ε is due to the nature of near fields, where electric and magnetic fields are decoupled; for our choice of polarization, μ=-1 is the only stringent condition for near-field focusing. The choice of ε=1 does, however, result in some artifacts being introduced on the sides of the image. Note also that the change in the reflectance properties of the slab also results in more power being coupled through the slits, so that the overall image intensity is larger than in the other cases.

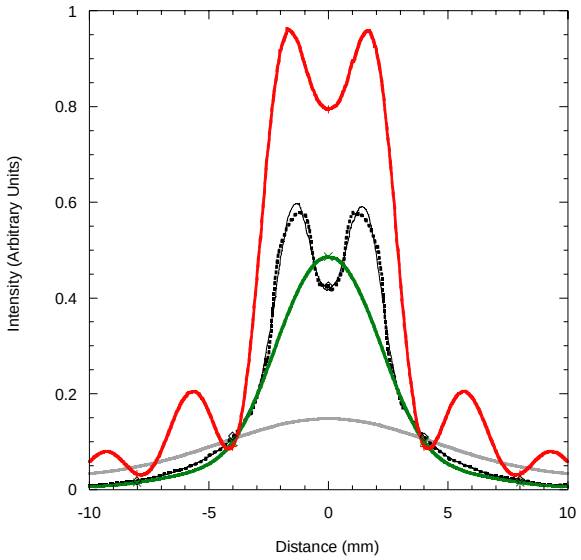

Fig. 5. Field intensity plots along the image plane after the slab. Black dashed curve: the object distribution. Gray curve: after insertion of a dielectric slab with ε=2.2. Black solid curve: after insertion of a slab with ε=-1+0.001i and μ=-1+0.001i. Green curve: after insertion of a slab with ε=-1+0.1i and μ=-1+0.1i. Red curve: after insertion of a slab with ε=+1+0.001i and μ=-1+0.001i.

4. A negative index focusing lens

The geometrical optics associated with structures formed from negative index material are very different from structures formed from positive index materials. Veselago pointed out that a negative index material in the shape of a converging lens, for example, would act as a diverging lens, and vice versa [1]. This might appear at first to be uninteresting, as it there would seem to be no intrinsic advantage to an optic formed from a negative index material. However, a lens element formed from material with ε=μ=-1 has the singular advantage that it is matched to free space, yet can alter the trajectory of transmitted waves as if the material possessed a much larger index.

To illustrate this point, we have compared the focusing abilities of collimating lenses formed from negative and positive index materials. As a guide for our lens design, we determine the focal length utilizing the thin (cylindrical) lens approximation, which yields

#1998 - $15.00 US
Received January 17, 2003; Revised March 09, 2003

$$f = \left| \frac{R}{n-1} \right|. \quad (1)$$

In Eq. (1) f, the focal length, depends on the refractive index, n, and the radius-of-curvature of the lens surface. The absolute value is taken, as there is an overall sign change when the lens is converging versus diverging. Note that a concave cylindrical (thin) lens with n=-1 has the same focusing properties as a convex (thin) lens with n=+3.

The similarities between the positive and negative index lenses can be seen by comparing Figs. 6(a) and 6(b). Figure 6(a) shows a collimated beam incident on an n=+3 lens with radius of curvature R=6 cm. From Eq. (1), the focal length is predicted to be f=R/2, or 3 cm, in agreement with that found in Fig. 6(a) despite being far away from the geometrical optics regime. A collimated beam incident on an n=-1 cylindrical lens is shown in Fig. 6(b), where it can be seen that the resulting focal length and field intensity distribution are nearly identical to the n=+3 lens.

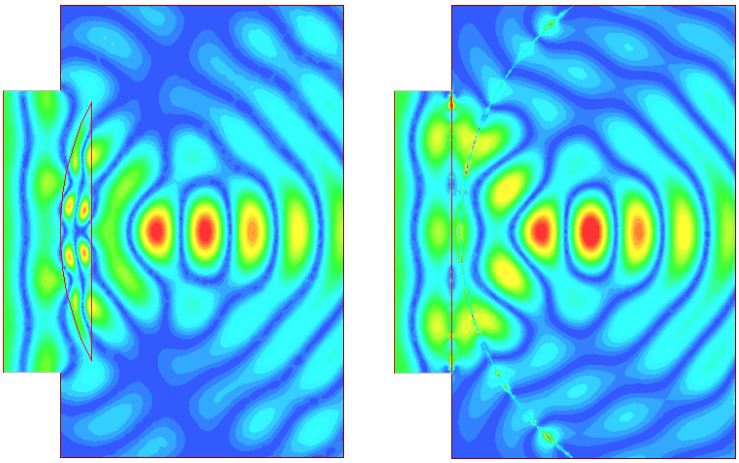

Fig. 6. (a) A wave incident on a positive index (n=+3) converging lens with R=6 cm is focused to a spot 3 cm away. (b) Similarly, a wave incident on a negative index (n=-1, ε=μ=-1) concave lens with R=6 cm is also focused to a spot 3 cm away. The wavelength used in the calculation was λ=3 cm.

5. Conclusion

Negative index materials have brought about a reconsideration of geometric and Fourier optics. We have numerically investigated the scattering of electromagnetic waves from several structures whose permittivity and permeability are both negative, and seen results consistent with the interpretation of a negative refractive index. In particular, we have shown that the exotic effects such as near-field regeneration and superfocusing predicted for negative refractive materials can be realized in negative index materials over a parameter range that should be achievable in metamaterials.

Most of the simulations presented here do not defy intuition; on the contrary, they support what has been or can be shown analytically assuming the material property of negative refractive index. Yet, analysis of the physical optics associated with negative refractive index materials can lead to surprising results—as in the case of the perfect lens. As we move toward understanding more complicated structures, perhaps including combinations of positively and negatively refracting materials or structures with non-regular shape, simulations such as these are crucial, as analytical techniques are typically limited to the simplest geometries. The consistency of the simulations presented here provides evidence that standard numerical packages will indeed be trustworthy when it comes to analyzing more complicated negative index structures.

#1998 - $15.00 US
Received January 17, 2003; Revised March 09, 2003

Acknowledgements

We are grateful to Sheldon Schultz (UCSD) and Minas Tanielian, Claudio Parazzoli and Bob Greegor (Phantomworks, Boeing) for helpful discussions. This work was supported by ONR (Contract No. N00014-01-1-0803) and DARPA via a grant through AFOSR (Contract No. 972-01-2-0016).

#1998 - $15.00 US Received January 17, 2003; Revised March 09, 2003